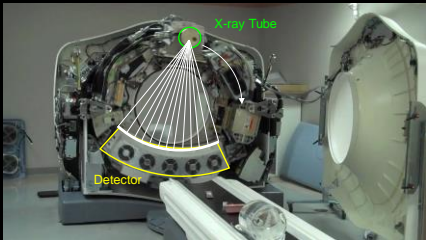


THE DEPARTMENT OF BIOMEDICAL ENGINEERING

Getting More Image Quality with Less Data in X-Ray CT

J. Webster Stayman
Advanced Imaging Algorithms and Instrumentation Lab (aiai.jhu.edu)
Johns Hopkins University
August 30, 2018

CT Hardware Basics

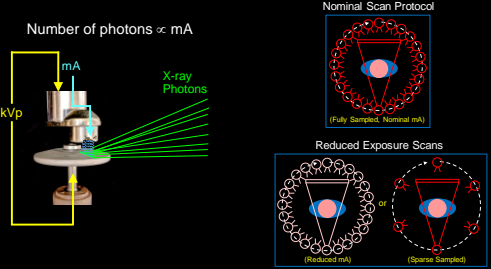


The diagram shows a cross-section of a CT scanner gantry. A green arrow labeled 'X-ray Tube' points to the source of the X-rays. A yellow arc labeled 'Detector' represents the array of detectors that capture the X-rays. The X-rays are shown as a fan beam passing through a patient (represented by a white cylinder) and hitting the detector.

(image Credit) <https://www.youtube.com/watch?v=bg0Inhw2ARw>

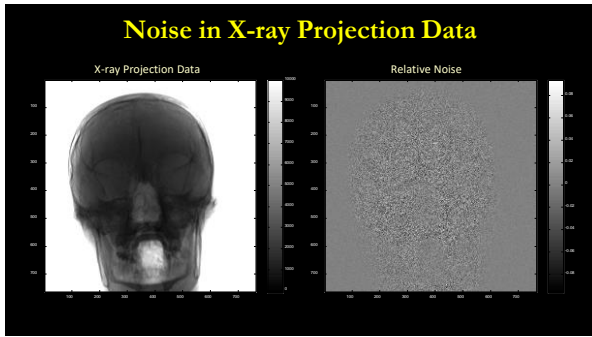
X-ray Tube Physics and Dose Reduction

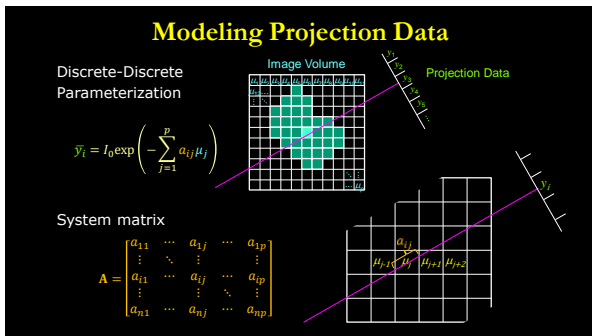
Number of photons \propto mA

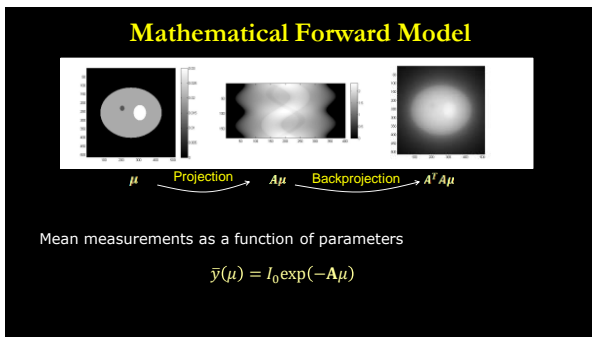


The diagram illustrates the relationship between X-ray tube parameters and dose reduction. On the left, a schematic shows an X-ray tube with 'kVp' and 'mA' labels, and 'X-ray Photons' being emitted. On the right, three circular diagrams represent different scan protocols:

- Nominal Scan Protocol:** (Fully Sampled, Nominal mA) - Shows a full circle of red dots representing a fully sampled scan.
- Reduced Exposure Scans:** (Reduced mA) and (Sparse Sampled) - Shows a partial circle of red dots, indicating reduced exposure and sparse sampling.

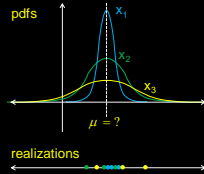






How to deal with unequal measurement noise (Simple Estimation Problem)

3 Random Variables
 Different std dev ($\sigma_1, \sigma_2, \sigma_3$)
 Best way to estimate μ ?

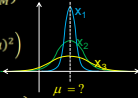


Maximum Likelihood Estimation

Find the parameter values most likely to be responsible for the observed data.

Likelihood Function $L(\mathbf{x}; \boldsymbol{\mu}) = p(x_1, x_2, \dots, x_N | \mu_1, \mu_2, \dots, \mu_M)$

$$L(\mathbf{x}; \mu) = p(\mathbf{x}|\mu) = \prod_{i=1}^3 p(x_i|\mu) \quad p(x_i|\mu) = \frac{1}{\sqrt{2\pi\sigma_i^2}} \exp\left(-\frac{1}{2\sigma_i^2}(x_i - \mu)^2\right)$$



Maximum Likelihood Objective Function $\hat{\boldsymbol{\mu}} = \operatorname{argmax} L(\mathbf{x}; \boldsymbol{\mu})$

$$\frac{\partial}{\partial \mu} \log L(\mathbf{x}; \mu) = \sum_{i=1}^3 \frac{1}{\sigma_i^2} (x_i - \mu) \quad \xrightarrow{\frac{\partial}{\partial \mu} = 0} \quad \hat{\mu} = \frac{\sum_{i=1}^3 \frac{x_i}{\sigma_i^2}}{\sum_{i=1}^3 \frac{1}{\sigma_i^2}}$$

Maximum Likelihood Estimation for CT

Log transformed data case (e.g. $l = -\log \left[\frac{y}{\sigma_0} \right]$)

$$l(\mu) = A\mu \quad P_{l_i} = \frac{1}{\sqrt{2\pi\sigma_i^2}} \exp\left(-\frac{1}{2\sigma_i^2}(l_i - l(\mu))^2\right)$$


Likelihood-based Objective $\log L(\mathbf{y}; \mu) = -\sum_{i=1}^N \frac{1}{2} \log(2\pi\sigma_i^2) - \sum_{i=1}^N \frac{1}{2\sigma_i^2} (l_i - A\mu)^2$

$$\equiv -[l - A\mu]^T \mathbf{D} \left[\frac{1}{\sigma_i^2} \right] [l - A\mu] = -\|l - A\mu\|_{\Sigma}^2$$

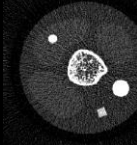
Solve for μ $\hat{\mu} = \operatorname{argmax} \log L(\mathbf{y}; \mu) = \left[\mathbf{A}^T \mathbf{D} \left[\frac{1}{\sigma_i^2} \right] \mathbf{A} \right]^{-1} \mathbf{A}^T \mathbf{D} \left[\frac{1}{\sigma_i^2} \right] l$

Statistical vs Nonstatistical Reconstruction

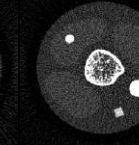
Ground Truth



Nonstatistical Method
(FBP, ART, etc.)



Statistical Method
(Maximum-Likelihood)



Statistical methods weigh important of individual data points
BUT noise control requires additional information

Additional Information through Regularization

Integrating information via a change in the objective function

$$\hat{\mu} = \operatorname{argmax}_{\mu} \log L(y; \mu) - \beta R(\mu)$$

Penalized-Likelihood Estimation

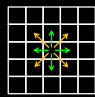
Choices of regularization $R(\mu)$

- Local smoothness
- Edge-preservation
- Prior images
- Patches/dictionaries/learned regularization

Regularization of Local Image Properties

Pairwise Penalty

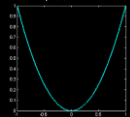
$$R(\mu) = \sum_{j, k \in \mathcal{N}} w_{jk} \psi(\mu_j - \mu_k)$$



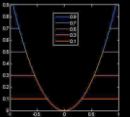
$k_{\text{row}} = \begin{bmatrix} -1 & -1 & -1 \\ -1 & 4 & -1 \\ -1 & -1 & -1 \end{bmatrix}$
 $k_{\text{2nd}} = \begin{bmatrix} -1 & -1 & -1 \\ -1 & 4 & -1 \\ -1 & -1 & -1 \end{bmatrix}$

Penalty Choices

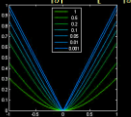
Quadratic

 $\psi(t) = t^2$


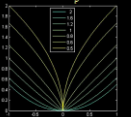
Truncated Quadratic

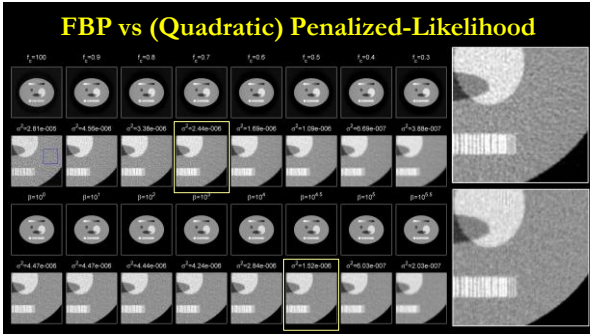
 $\psi(t; \delta) = |t|^2_{\delta}$


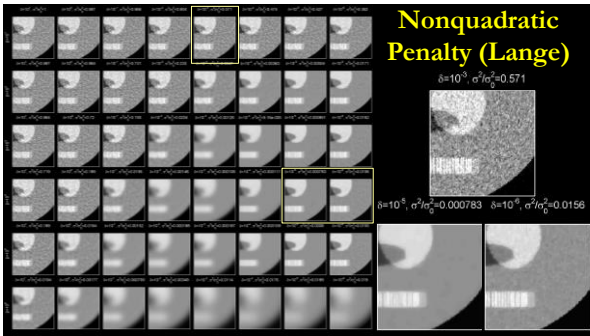
Lange

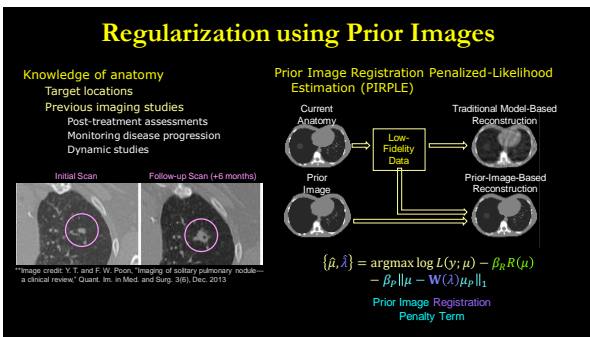
 $\psi(t; \delta) = \delta \left[\frac{t^2}{\delta} + \log \left(1 + \frac{t^2}{\delta} \right) \right]$


P-norm

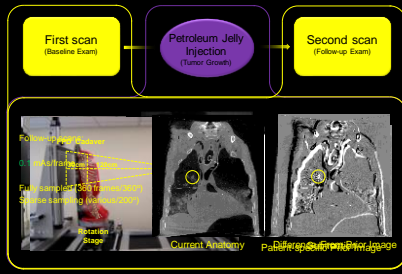
 $\psi(t; p) = \frac{1}{p} |t|^p$




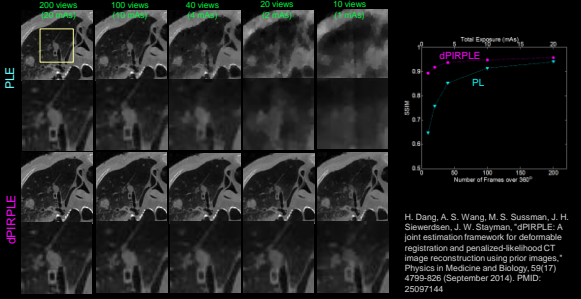




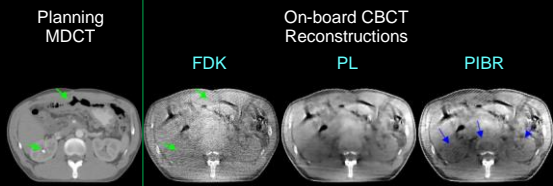
Prior Image Regularization Experiments



Dose reduction in Lung Nodule Surveillance



Prior Images for Image Quality Improvement



H. Zhang, G. J. Garg, J. Lee, J. Wong, J. W. Stayman, "Integration of prior CT into CBCT reconstruction for improved image quality via reconstruction of difference: first patient studies," *Proc. SPIE Medical Imaging Orlando, FL, March 2017*, 10132: 1-6.

Regularization using Patches/Dictionaries

General/learned knowledge of image features
 Need a dictionary of features/patches
 Sparse representations,
 linear combinations of few patches

Objective Function
 $\{\hat{\mu}, \hat{\lambda}\} = \operatorname{argmax}_{\mu, \lambda} \log L(y; \mu)$

$$-\beta \left(\sum_p \|E_p \mu - D \lambda_p\|_2^2 + \sum_p v_p \|\lambda_p\|_0 \right)$$

Images adapted from: Q Xu, H Yu, X Mou, L Zhang, J Hsieh, G Wang, "Low-dose x-ray CT reconstruction via dictionary learning," *IEEE Trans. Medical Imaging*, 31(9), September 2012.

Dictionary Methods & Few View Reconstructions

Image credits: Q Xu, H Yu, X Mou, L Zhang, J Hsieh, G Wang, "Low-dose x-ray CT reconstruction via dictionary learning," *IEEE Trans. Medical Imaging*, 31(9), September 2012.

Additional Information in the Forward Model

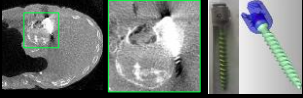
$$\bar{y}(\mu) = I_0 \exp(-A\mu)$$

Forward model has many simplifications in physics...
 Model ignores
 Scatter
 Spectral effects
 Focal spot blur
 Detector blur

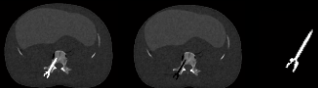
Object model may have constraints
 Nonnegativity
 Known element/components in the field-of-view

Modeling Known Components in the Object

Implants
 Susceptible to metal artifacts
 Strongest near the device
 Region-of-interest is near implant



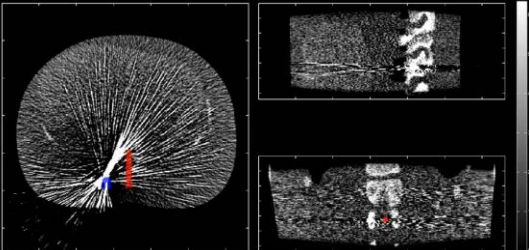
Include a component model in explicitly in the object model

$$\mu(\mu_{\text{anatomy}}, \lambda) = \mathbf{D}(\mathbf{W}(\lambda)\mathbf{m})\mu_{\text{anatomy}} + \mathbf{W}(\lambda)\mu_{\text{implant}}$$


J. W. Stayman, Y. Otake, J. L. Prince, J. H. Siewerdsen, "Model-based Tomographic Reconstruction of Objects containing Known Components,"
 IEEE Trans. Medical Imaging, 31(10), 1837-1848 (October 2012), PMID: 22614374

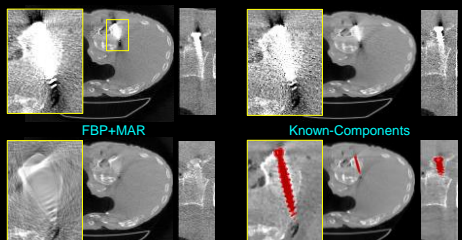
Known Component Reconstruction Iterations

Iter #0



Reconstructions of an Implanted Cadaver

FBP Penalized-Likelihood



FBP+MAR Known-Components

S. Xu, A. Uneri, A. J. Khanna, J. H. Siewerdsen, J. W. Stayman, "Polyenergetic known-component CT reconstruction with unknown material compositions and unknown x-ray spectra," Physics in Medicine and Biology, 62(8), 3352-74 (April 2017)

Improving the Physical Model (Focal Spot Blur)

$$\bar{y}_i = \sum_{k=1}^K b_{ik} \exp \left(- \sum_{j=1}^p a_{kj} \mu_j \right)$$

Improved Physical Modeling (Focal Spot)

S. Tilley II, W. Zbijewski, and J. W. Stayman, "High-Fidelity Modeling of Shift-Variant Focal-Spot Blur for High-Resolution CT" in *The 14th International Meeting on Fully Three-Dimensional Image Reconstruction in Radiology and Nuclear Medicine*, 2017, pp. 752-759.

CT Reconstruction Summary

Advanced Reconstruction Aims
 Dose reduction, improved image quality

CT Forward Model
 Nonlinear, but often linearized
 Measurement statistics are important (SNR varies widely)
 Advanced physical modeling permits image quality improvements

CT Regularization Strategies
 Standard smoothness and edge-preservation
 Use of prior images (e.g., sequential studies)
 Generalized dictionary methods including machine learning

Other Objective Function Modifications
 Additional constraints on the object (e.g., known components)

Acknowledgements

Advanced Imaging
Algorithms &
Instrumentation
Laboratory



AIAI Laboratory
Advanced Imaging Algorithms
and Instrumentation Lab
aiai.jhu.edu
stayman@gmail.com

Faculty and Scientists

Grace Gang (AIAI)
Amir Pormorteza (AIAI)
Jeffrey Siewerdsen (I-STAR)
Alejandro Sisniega (I-STAR)
Adam Wang (I-STAR)
Shiyu Xu (AIAI)
Wojciech Zbijewski (I-STAR)
Hao Zhang (AIAI)

Clinicians

John Carey - Otolaryngology
Kelvin Hong - (Interventional) Radiology
Satomi Kawamoto - Radiology
A Jay Khanna - Orthopaedic Surgery
Eleni Liapl - Radiology
Tony Lin - Radiology
Martin Radvany - (Interventional) Radiology
Marc Sussman - Thoracic Surgery
Clifford Weiss - (Interventional) Radiology
John Wong - Radiation Oncology

Students

Hao Dang
Juliana Carneiro Gomes
Andrew Mao
Gabriela Rodal
Saeed Seyyedi
Steven Tiley II
Ali Uneri
Wenyang Wang
Chengzhu Zhang
Esme Zhang

Funding/Support

NIH: U01EB014964, R01EB025470, R21CA219608, R21EB014964, KL2TR001077, R01CA112163
Academic-Industry Partnerships: Siemens, Varian Medical Systems, Elekta AB, Carestream Health
Research Partnership/Agreements: Philips Healthcare, Canon Medical

This work was supported, in part, by the above grants. The contents of this presentation are solely the responsibility of the authors and do not necessarily represent the official view of Johns Hopkins, the NIH, or other organizations.
